Evaluation of a compact CCD-based high-resolution autocollimator for use as a slope sensor

Rohan Isaac

August 11, 2012

Abstract

We evaluate the feasibility of high-resolution CCD-based autocollimator for use as a slope sensor. The compact autocollimator is based on a CCD detector with a small probe beam. We also explore several methods of determining the centroid of a laser beam spot to sub-pixel accuracy, and develop MATLAB and C++ software to calculate these values. The centroid algorithm developed is also used in aligning a laser for the Long Trace Profiler (LTP).

1 High-resolution slope sensor

1.1 Introduction

The Advanced Photon Source at Argonne National Lab generates high energy x-ray beams for use in experiments in a variety of fields. One of the ways to focus x-rays to the diffraction limit is using Kirkpatrick-Baez (KB) mirrors[1]. This system uses two elliptical cylindrical mirrors arranged in a cross mirror geometry to focus x-rays (See figure 1).These mirrors require a high degree of smoothness to preserve the properties of the source beam. Surface irregularities exceeding 0.2 micro radian rms slope error will cause the focused beam profile to broaden and decrease its peak intensity[7]. Mirror profiles are measured using a Long Trace Profiler – an instrument for measuring directly the slope of optical surfaces over long trace lengths[8]. The aim of this project is to test the feasibility of a CCD-based autocollimator with a small probe beam with a goal to achieve a resolution of less than 50 nano radians for potential use in an LTP. We based our setup on a scheme described in a paper by Kuang, Hong, and Feng [2].

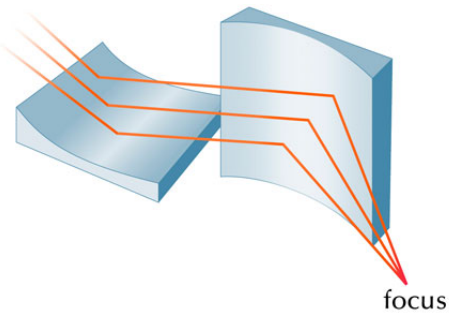

Figure 1: Kirkpatrick-Baez mirror setup to focus x-rays. [Soure: SLAC National Accelerator Laboratory]

1.2 Basic Principle of Autocollimators

Autocollimators use a collimated beam reflected off a plane surface such as a mirror to measure small angles with high precision. If the mirror is not completely perpendicular to the projected beam, the reflected beam takes a different path than the projected one. The deviation of the reflected beam can be measured by focusing the beam onto a detector, and measuring the difference in its position compared to a undeviated beam. The deviation (Δ) of the reflected beam can be used to infer the angle of the mirror (θ) using the fundamental relation of autocollimators

$$\Delta = F \tan 2\theta \tag{1}$$

where F is the focal length of the lens used. Using the small angle approximation this can be reduced to

$$\theta = \frac{\Delta}{2F} \tag{2}$$

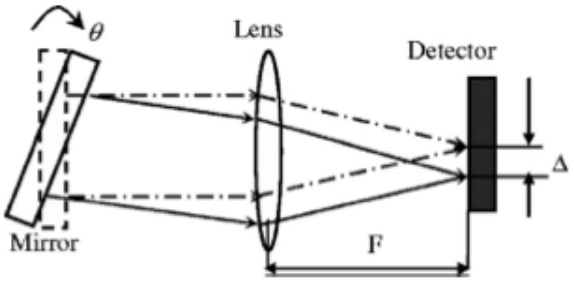

Figure 2: Fundamental Principle of Autocollimators [Source: Kuang, Cuifang, En Hong, and Qibo Feng]

1.3 Setup

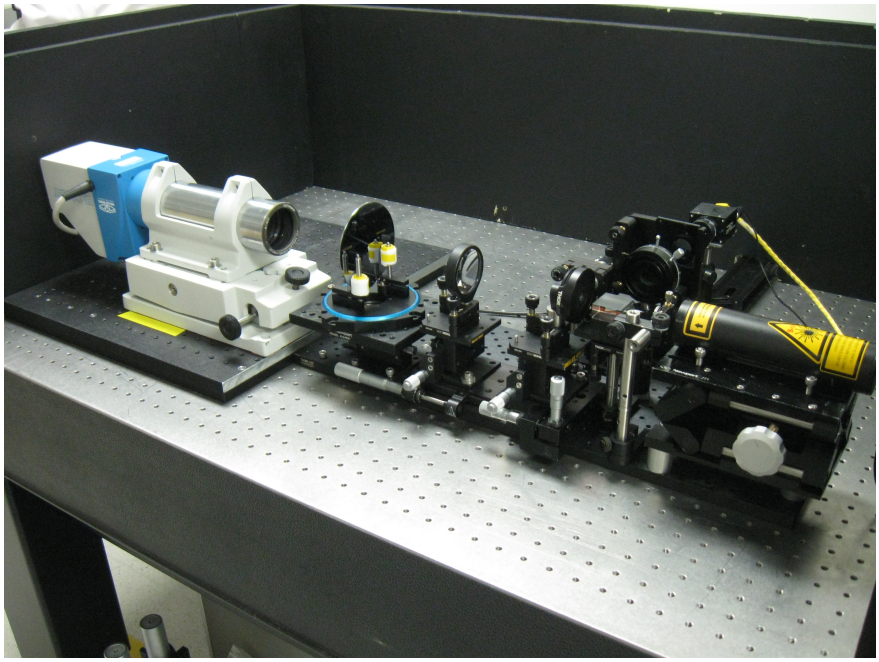

Figure 3: Our setup pointed at the test mirror, placed opposite to commercial autocollimator.

Our setup consisted of beam of light emitted from an randomly polarized 5mW 632.8nm HeNe Laser (Thor Labs HRR005). This beam is passed through a linear polarizer adjusted in such a manner that the beam travels straight through a polarizing beam splitter. After this, the beam traverses through a quarter plate, that makes the linearly polarized light become circularly polarized. This beam then passed through a pair of collimating lenses ($f = 10$mm and $f = 100$mm respectively) to the mirror. The beam after being reflected off the surface of the mirror passes back though the lenses and the quarter wave plate. This returns the beam back to being linearly polarized, but its phase is shifted by 90°, so this time it gets reflected by the beam splitter to the perpendicular components. This beam is then passed through another linear polarizer as well as a neutral density filter to control its intensity, before passing through another pair of lenses ($f = 50$mm and $f = -6$mm)that focus the beam on the sensor of the CCD camera.

The collimation of the beam produced through the $f = 10$mm and $f = 100$mm lenses was verified using a bilateral image shearing interferometer, the 633 nm ParaLine Collimation Tester. The entire setup was mounted on a breadboard which was placed on an optical table for stability. Moreover, the setup was placed in an enclosure, to prevent distortion from stray light and airflow.

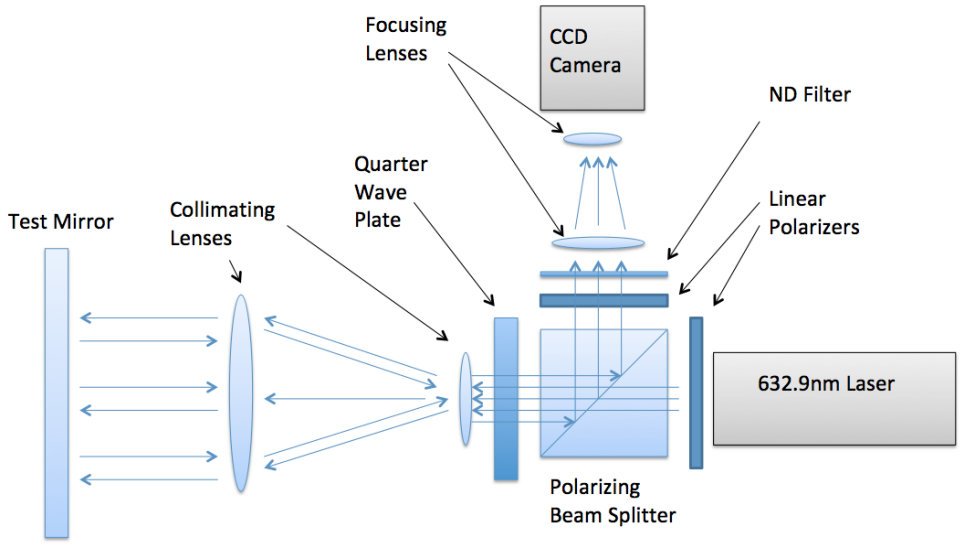

Figure 4: Schematic layout of our setup

1.4 Measurement principle

The two sets of combination lenses, one in front of the mirror and one in front of the CCD, are used to both increase the angular resolution of the system, as well as reduce the total installation space.

The size of the beam after collimation (d_2) is given by the equation

$$d_2 = \frac{f_2}{f_1} d_1 \tag{3}$$

Since $f_2 = 100\text{mm}$ and $f_1 = 10\text{mm}$, the collimating lenses set up in front of the test mirror increase the beam size by a factor of 10. This increases the beam diameter from 0.57mm to 5.7mm.

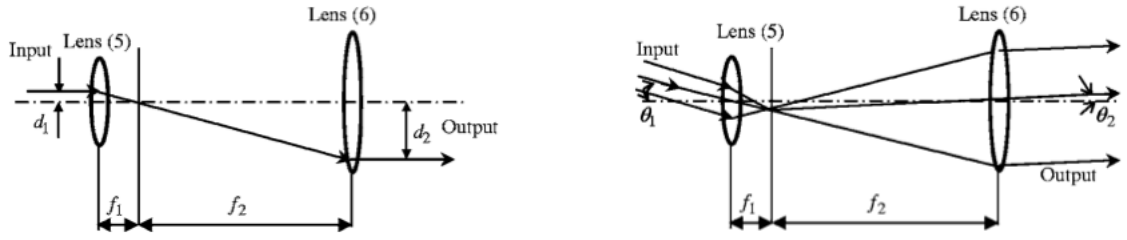

(a) Increase in beam size

(b) Increase in angular resolution

Figure 5: [Source: Kuang, Cuifang, En Hong, and Qibo Feng]

The angular change in the beam path after collimation, on the other hand is given

by

$$\theta_2 = \frac{f_1}{f_2}\theta_1 \tag{4}$$

This means for a small change in the angle of the mirror (θ_2), θ_1 will be amplified by a factor of 10. So the first pair of lenses increases the angular resolution by a factor of 10.

The second set of lenses in front of the CCD helps increase the angular resolution while decreasing the installation space. By changing the distance between the lenses (D_1) and the distance from the second lens to the CCD sensor (D_2), using the following relations derived from geometrical optics we can increase the equivalent focal length (f), while decreasing the total size(D). From (2), we know that f is directly proportional to the resolution. In our setup, $f_3 = 50$mm, $f_4 = -6$mm and $D_1 = 59$mm, which gives $D_2 = 18$mm from (5), $D = 77$mm from (7), and $f = 100$mm from (6).

$$D_2 = f_4(f_3 - D_1)/(D_1 - f_3 + f_4) \tag{5}$$

$$f = f_3 f_4/(D_1 - f_3 + f_4) \tag{6}$$

$$D = D_1 + D_2 \tag{7}$$

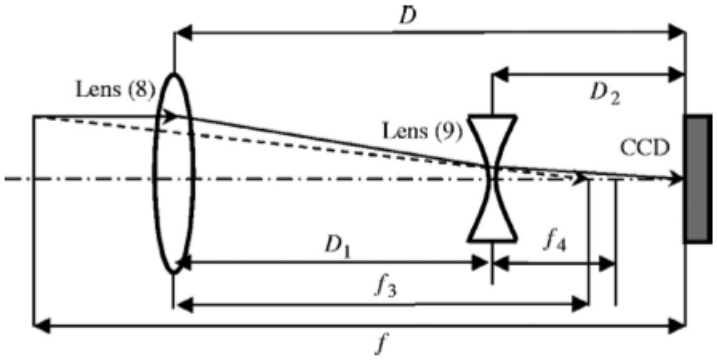

Figure 6: Lenses in front of the CCD increase the focal length f and thus the angular resolution, but while decreasing the installation space D [Source: Kuang, Cuifang, En Hong, and Qibo Feng]

1.5 Data Acquisition

The primary data from our system was acquired through the Allied Vision Prosilica GC2450 high resolution CCD. We acquired 100 frames of data at 2448×2050 (5MP) resolution in 8-bit grayscale TIFF images using an automation script for each position

we tested. The frames we then averaged using a basic MATLAB routine in double precision data to give more accurate readings as well as to reduce noise levels.

1.6 Data Processing

To get nano radian precision using this system we need to determine the position of the focused beam to within sub pixel accuracy. The beam appears on the CCD as a spot which can be modeled as a 2D Gaussian function. There are a number of popular techniques that we can use to find the center of this beam spot. To this end we tested and compared some of the popular algorithms with a simple simulation written in MATLAB code. The results of the simulation as well as the comparison of the techniques are detailed in Section 2. The method that we used was the Fourier methods described in Section 2.2, which locates the centroid of a beam to an accuracy of up to 0.024px [5].

A 1 pixel deviation of the beam on the camera sensor corresponds to 3.45μm, and by using the formulas (2), (4) and (6), we can see that this deviation gives us an angular resolution of 1.725μrad/pixel. Since we have sub-pixel resolution of the centroid of the beam spot up to a precision of 0.024px [5], the total theoretical resolution of of the system is 41.4 nano radians.

1.7 Testing and Results

To test the precision of the system we used, we used a commercial autocollimator made by MOLLER-WENDEL, the ELCOMAT 2000. The mirror we used for testing was a $\sim$ 100mm diameter silicon mirror that was polished on both sides to a surface roughness less than 7Å. This mirror was mounted on a compact ultrasonic pizeo motor driven rotation stage (Physik Instrumente M-660). We placed our system on one side of the mirror, and the commercial autocollimator on the other side, aligned so that any angular deviation of the mirror would be reflected equally on both systems.

For each data point in the test, we rotated the stage by 0.01 degrees (about 174.5μrad) and took data from both systems. For data from the commercial autocollimator, we connected it to a computer using a RS232 serial port and acquired 4 kilobytes of data (about 500 data points of x and y angular position) for each point using a LabView interface. The binary data was decoded using a custom C++ program written using scheme described by manufacturer, and averaged. The standard deviation of the data points was less than 0.003 arc seconds (10 nano radians) in all cases.

From our results (Figure 7) we note that while the principle of the setup works very well, as we have a strongly linear relation between the two autocollimators (R = .998), our error is very large (average error of 24 micro radian). This is mainly due to

the difficulty of aligning the optical setup on our bench to precisely focus on the CCD sensor, as well as the reflections and other noise incident on the sensor which reduce the effectiveness of the centroid algorithm used.

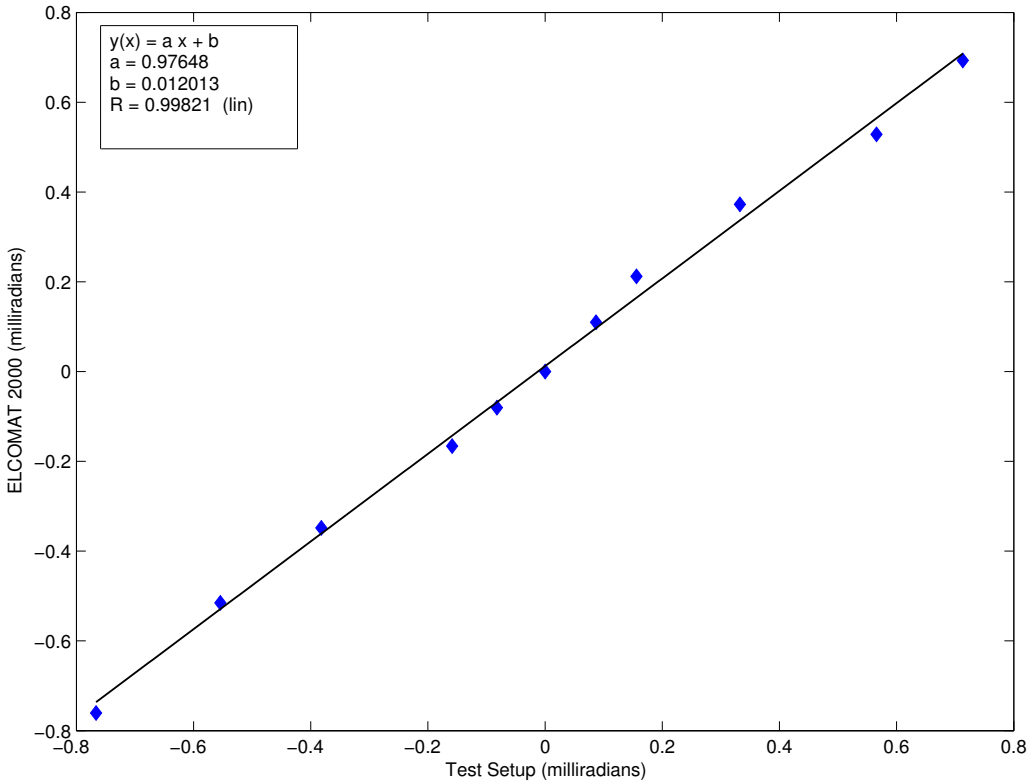

Figure 7: Results of the relation between the ELCOMAT2000 and our test setup

2 Comparison of methods to detect centroid of a Gaussian laser beam spot

Our results in the previous section hinge on our ability to find the centroid of the beam to within sub pixel resolution. Thus we studied a number of popular methods, and ran simulations to test the effectiveness of each method. The details of the methods as well as their advantages and disadvantages are given below.

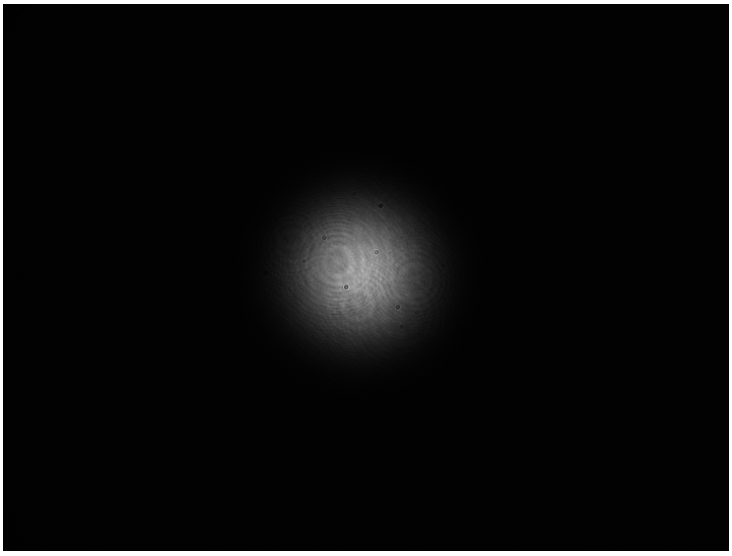

Figure 8: Single frame of laser beam incident on CCD

2.1 Center of Mass

The center of mass method of determining center of spot is a very straightforward method of determining the center of the laser spot. The intensities (I) of each pixel with coordinates (x,y) are treated as mass values, and the center of mass is then determined using the equations[5]:

$$x_c = \frac{\int_\infty^\infty \int_\infty^\infty xI(x,y)dxdy}{\int_\infty^\infty \int_\infty^\infty I(x)} \tag{8}$$

$$y_c = \frac{\int_\infty^\infty \int_\infty^\infty yI(x,y)dxdy}{\int_\infty^\infty \int_\infty^\infty I(x)} \tag{9}$$

This center of mass represents the position of the beam spot, similar to the way the center of mass of a physical body is the point on the body where all the mass

can be said to be concentrated. However, since intensity is analogous to mass, any intensity contributes to the weight, which means that noise and other irregularities affect the location of the center of mass, which is problematic. This method gives us a measurement error of 0.038px[5].

2.2 Fourier Method

The Fourier method described below alleviates many of the drawbacks of the center of mass methods. The main principle of the method is using the Fourier transform of the profile to find a position at which the antisymmetric portion of the transform is minimal. Another advantage of this technique is the high frequency components of the profile can be filtered out, which usually represent the disturbances in the profile such as noise et cetera.

The algorithm for a one dimensional profile is as follows[3]. If a real profile $f(x)$ is defined at $2N$ discrete points, the Fourier series of the profile is given by

$$F(x) = \sum_{k=-N}^{N} C_k e^{2\pi ikx/N} \tag{10}$$

where the complex Fourier coefficients are given by $C_k = A_k + iB_k$, and $C_k = C^*_{-k}$

The imaginary component of the Fourier series represents the measure of asymmetry of the signal centered around the origin, and can be represented as

$$A = \sum_{k=-N}^{N} [\mathrm{IM}(C_k)]^2 \tag{11}$$

If we consider a function where the origin is shifted by a distance Δx i.e. $f(x-\Delta x)$, the Fourier series of the function is given by

$$F(x - \Delta x) = \sum_{k=-N}^{N} C_k e^{-2\pi ik\Delta x/N} e^{2\pi ikx/N} \tag{12}$$

and the corresponding asymmetry is

$$A(\Delta x) = \sum_{k=-N}^{N} \left[\mathrm{IM}[C_k e^{-2\pi ik\Delta x/N}]\right]^2 \tag{13}$$

For an ideal or symmetric profile such as the Gaussian bell profile, the maximum of the fundamental oscillation is simultaneously the axis of symmetry of the profile, with all other higher order components symmetric to this axis. The high order components also contain imperfections in the measurement of the profile such as noise and other imperfections. For these reasons we limit ourselves the fundamental frequency $k = 1$.

The fundamental frequency is symmetric when

$$\mathrm{IM}[C_1 e^{-2\pi i \Delta x/N}] = A_1 \sin(2\pi\Delta x/N) - B_1 \cos(2\pi\Delta x/N) = 0 \tag{14}$$

Using definitions of C_k and e^x we can simplify to show

$$\Delta x = \frac{N}{2\pi}\left(\arctan\left(\frac{B_1}{A_1}\right) + \Phi\right) \tag{15}$$

This method gives us an error of 0.024 pixels[5], which is about 33% more accurate than the Center of Mass method.

2.3 2D Gaussian curve fitting

While an ideal scenario would involve fitting a 2D gaussian profile to the image, in practice, finding the best fit for a gaussian function on an image is a very computationally expensive task, taking far longer than the other two methods [5], so we did not explore this method.

2.4 Results

We tested implementation of both the Center of Mass method as well as the Fourier method in MATLAB on a number of simulated images, generated using a simple 2D Gaussian profile. The base case of our test image was a 2500×2000px image with a 2D Gaussian function centered at $x_0 = 1000$px, $y_0 = 1000$px with a spread $\sigma_x = \sigma_y = 50$ pixels. The function was also given an amplitude of $A = 100$ in arbitrary units.

$$f(x,y) = A \exp\left(-\left(\frac{(x-x_o)^2}{2\sigma_x^2} + \frac{(y-y_o)^2}{2\sigma_y^2}\right)\right) \tag{16}$$

We looked at the performance of each algorithm as a function of the following parameters.

1. Amplitude of Gaussian
2. Noise Intensity
3. Spot size (Gaussian spread)
4. Addition of secondary spot.

We noticed in all these cases the, Fourier method performed as well as or better than the Center of Mass method. The Center of Mass method performed exceptionally poorly in the case of significant noise, where the additional weights from the noise greatly skewed the result. This methods also deteriorated when the Gaussian function spread beyond the bounds of the image (e.g. with large spot size or high intensities) as this method could not account for the information lost.

The one advantage of the center of mass methods is it speed, as it performed twice as fast as the Fourier method. This difference is negligible however, as MATLAB implementations of both algorithms can be run under 10milliseconds on our 8-core

Intel i7 workstation. We also developed C++ versions of our code for fast operation as well as easy deployment on other machines.

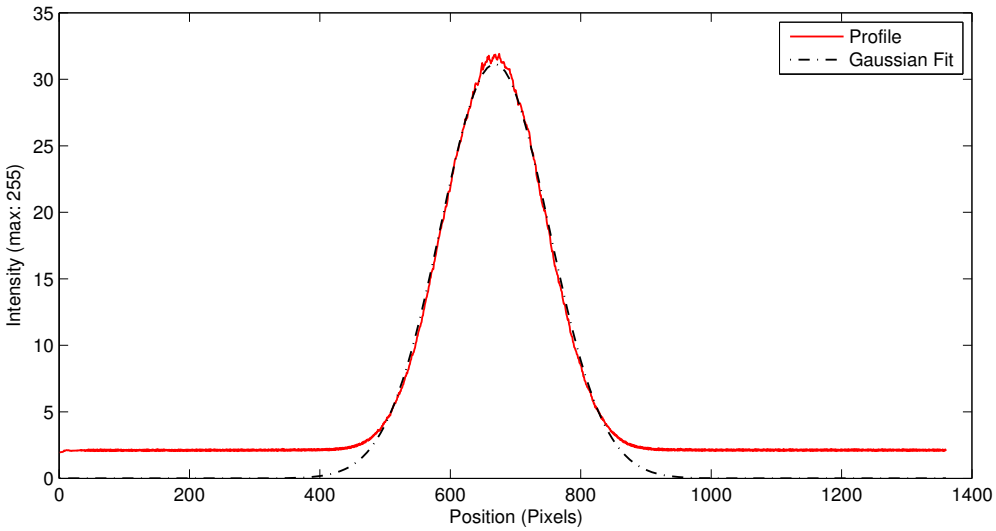

Figure 9: Profile of beam shown in Figure 8 exhibiting Gaussian nature.

3 Alignment of Long Trace Profiler laser

We used the centroid detection system we developed for the autocollimator slope sensor to help us align the laser on the long trace profiler. We captured frames of data from a CCD which was set up in the path of the laser beam on the traveling mount of the LTP. We then moved the mount over 1000mm while capturing frames about every 4.5mm. We then plotted the position of the centroid of the beam spot in both the x and the y directions over the course of the motion of the long trace profiler. For each axis, we adjusted the position of the laser and collected data, and repeated this process until we minimized the deviation of the centroid along that axis.

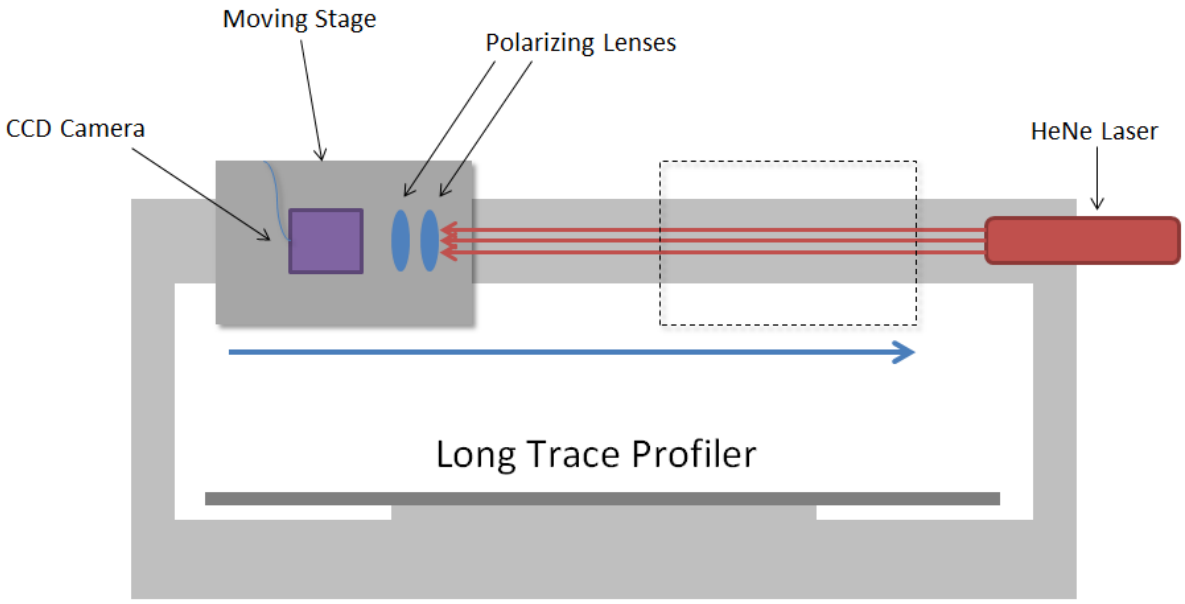

Figure 10: Schematic showing application to Long Trace Profiler.

Since the laser beam is very susceptible to distortions from airflow and temperature gradients, especially over longer distances, we performed this alignment in a controlled environment. We also averaged as many as 10 scans together to further minimize the effect of these distortions on our data.

We also looked at the effect of the intensity of the laser beam in getting reliable data for the experiment described above. We adjusted the intensity of the beam falling on the sensor of the CCD (Allied Vision Prosilica GC1380H 1360px $\times$ 1024px) using a system of two linear polarizers. We found that for low intensities, the intensity variation across the length of the system was large, and this affected the accuracy of the centroid detection scheme. For high intensities, this variation is not as pronounced, and this leads to better stability in the data.

3.1 Results

Before adjusting the alignment of the laser, reference data was taken to test how far the beam deviated over a length of 1000mm. This was compared with the results of the system after alignment and found to be over a three-fold improvement in both the x and the y axis. At this point, however we were limited by the mechanical limitations of our alignment system, and were unable to further improve it's alignment.

Table 1: Results of laser alignment

Before Alignment		After Alignment	
Δx	5.688px (0.0367mm)	Δx	1.555px (0.0100mm)
Δy	6.316px (0.0407mm)	Δy	2.037px (0.0131mm)
θx	36.687 micro radian	θx	10.027 micro radian
θy	40.740 micro radian	θy	13.141 micro radian

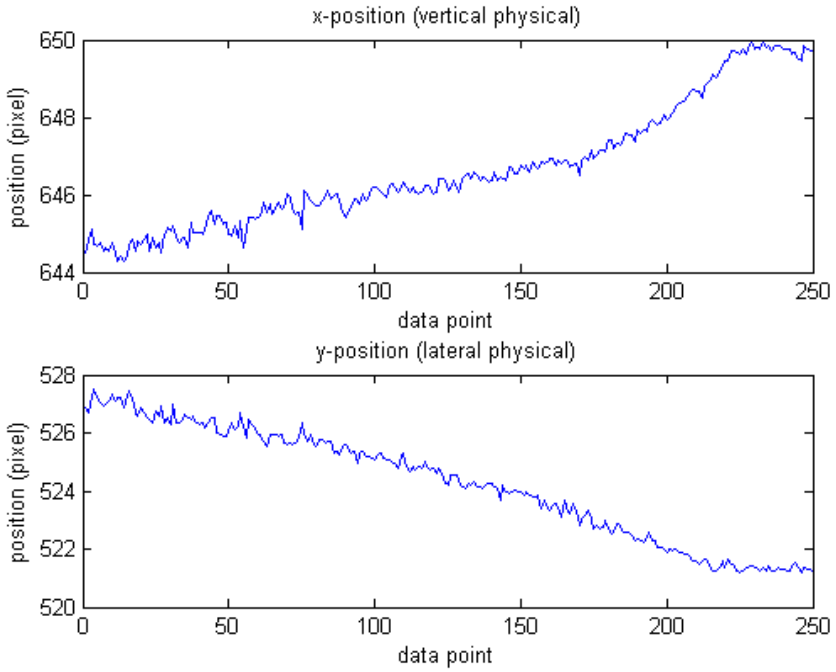

Figure 11: Deviation of the centroid of the beam over 1000mm before alignment

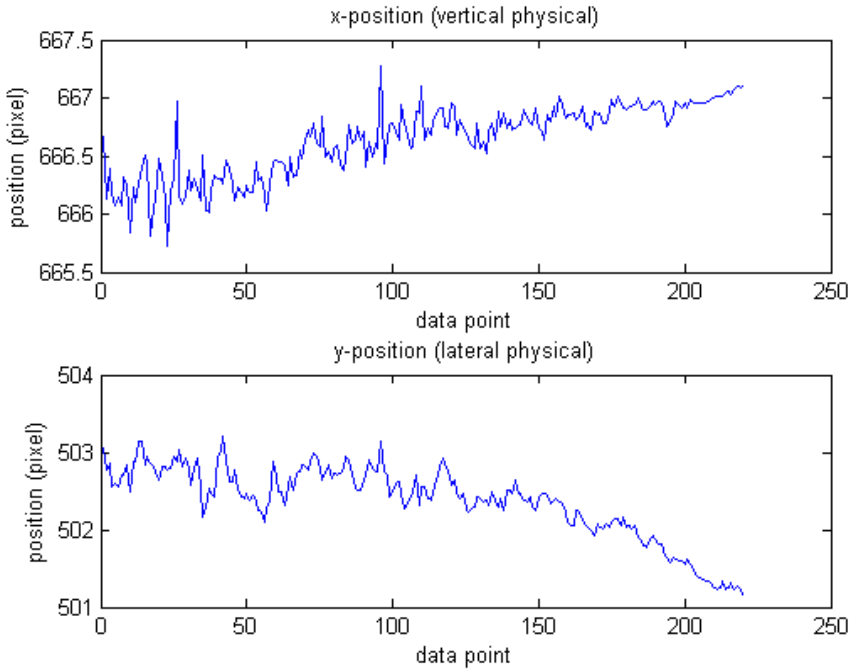

Figure 12: Deviation of the centroid of the beam over 1000mm after alignment

4 Conclusions

We were able to test the high-precision CCD-based autocollimator setup described. While our results did not give us the resolution we were aiming for, the basic principles of the system still hold. Future work in this topic might include designing a custom built housing for the system, which could further minimize environmental effects such as temperature variations, airflow, and stray light. The resolution could also be enhanced by a longer effective focal length or higher spatial resolution in the CCD sensor. The centroid algorithms we developed play a key role in this system, and also have many other applications, as seen in the alignment of the LTP laser.

5 Acknowledgements

The research was conducted with the Optics group at the Advanced Photon Source at Argonne National Lab, Lemont, IL, USA. I am grateful to my mentor, Dr. Lahsen Assoufid, for his help and guidance during this internship. I would also like to thank Dr. Shashidhara Marathe, Dr. Bing Shi, Jun Qian and John Attig and other members of the optics group for their help in this project. I would like to extend my thanks to the Lee Teng Internship program, especially to Dr. Eric Prebys and Dr. Linda Spentzouris.

References

[1] Suzuki, Yoshio, and Fumihiko Uchida. "X-Ray Focusing with Elliptical Kirkpatrick-Baez Mirror System." *Japanese Journal of Applied Physics* 30.Part 1, No. 5 (1991): 1127-130. Print.

[2] Kuang, Cuifang, En Hong, and Qibo Feng. "High-accuracy Method for Measuring Two-dimensional Angles of a Linear Guideway." *Optical Engineering* 46.5 (2007): 051016. Print.

[3] Weißhaar, Eckhard, Gerd Küveler, and Michele Bianda. "Schnelle Und Genaue Methode Zur Schwerpunktfindung in Messreihen." *Photonik* (2003): n. pag. Print.

[4] Alexander, Brian F. "Elimination of Systematic Error in Subpixel Accuracy Centroid Estimation." *Optical Engineering* 30.9 (1991): 1320. Print.

[5] Canabal, Héctor, José Alonso, and Eusebio Bernabeu. "Laser Beam Deflectometry Based on a Subpixel Resolution Algorithm." *Optical Engineering* 40.11 (2001): 2517. Print.

[6] Hou, Bo, Z. Y. Wu, J. L. De Bougrenet De La Tocnaye, and P. Grosso. "Charge-coupled Devices Combined with Centroid Algorithm for Laser Beam Deviation Measurements Compared to Position Sensitive Device." *Optical Engineering* 50.3 (2011). Print.

[7] Yamauchi, K., Yamamura, K., Mimura, H., Sano, Y., Saito, A., Souvorov, A., Yabashi, M., Tamasaku, K., Ishikawa, T. and Mori, Y. "Nearly diffraction-limited line focusing of a hard-X-ray beam with an elliptically figured mirror." *J. Synchrotron Rad* 9 (2002): 313-316. Print.

[8] Qian, Shinan, Werner Jark, and Peter Z. Takacs."The Penta-prism LTP: A Long-trace-profiler with Stationary Optical Head and Moving Penta Prisma)." *Review of Scientific Instruments* 66.3 (1995): 2562. Print.